Research Square

Preprints are preliminary reports that have not undergone peer review.
They should not be considered conclusive, used to inform clinical practice,
or referenced by the media as validated information.

An Antioxidative Sophora Exosomes Encapsulated Hydrogel Promotes Spinal Cord Repair by Regulating Oxidative Stress Microenvironment

Jiachen Chen
Institute of Pharmaceutics, College of Pharmaceutical Sciences, Zhejiang University
Jiahe Wu
Key Laboratory of Clinical Cancer Pharmacology and Toxicology Research of Zhejiang Province, Affiliated Hangzhou First People's Hospital, Zhejiang University School of Medicine
Jiafu Mu
Institute of Pharmaceutics, College of Pharmaceutical Sciences, Zhejiang University
Liming Li
Marine Life Research Center, Pilot National Laboratory for Marine Science and Technology
Jingyi Hu
Institute of Pharmaceutics, College of Pharmaceutical Sciences, Zhejiang University
Jian Cao
Institute of Pharmaceutics, College of Pharmaceutical Sciences, Zhejiang University
Jianqing Gao (gaojianqing@zju.edu.cn)
Institute of Pharmaceutics, College of Pharmaceutical Sciences, Zhejiang University
Hangjuan Lin
Ningbo Municipal Hospital of TCM, Affiliated Hospital of Zhejiang Chinese Medical University

Research Article

Keywords: Exosome, Rutin, Spinal cord injury, Microenvironment, Hydrogel

Posted Date: March 8th, 2022

DOI: https://doi.org/10.21203/rs.3.rs-1408741/v1

License: This work is licensed under a Creative Commons Attribution 4.0 International License.
Read Full License

Abstract

Background: Spinal cord injury (SCI) is recognized as a severe traumatic disease because of its complications and multiorgan dysfunction. After the injury, microenvironment stability disruption in the lesion will rapidly demolish the surrounding healthy tissues and cells via various pathways. Regulating the microenvironment is an effective strategy to mitigate the rigorous condition, which is beneficial for subsequent neural restoration and functional recovery. Nevertheless, sustained release, cellular uptake, and long-term retention in the impaired site of therapeutic molecules are insufficient.

Results: Herein, a local-implantation system is constructed for SCI treatment by encapsulating exosomes derived from *Flos Sophorae Immaturus* (so-exos) in a polydopamine (pDA) modified hydrogel (pDA-Gel). So-exos are applied as nano-scale natural vehicles of rutin, a flavonoid phytochemical that has been confirmed effective in microenvironment mitigation and nerve regeneration. pDA-Gel not only enables the long-term retention and sustainable release of so-exos in the lesion but also offers a nutritional and suitable microenvironment for nerve regeneration at the same time.

Conclusion: The pDA-Gel encapsulating so-exos exhibits rapid restoration of the nervous system and preservation of downstream urinary system by modulating the inflammatory and oxidative condition. The oxidative sophora exosome encapsulated hydrogel exhibits a potential SCI treatment via plant exosomes combinational delivery.

Introduction

Spinal cord injury (SCI) is a traumatic disease in the central nervous system. According to estimations, around half a million human beings suffer from SCI worldwide annually[1–3]. Prognoses are intended to be long-term physical impairments, especially with disability in the urinary, digestive, and locomotive systems[4]. Mortality and disability-adjusted life-years are remarkably harmed. Thus, global concerns have been paid in the intact recovery in the structure and function. In a primary injury, indigenous lesions and exogenous substances directly lose neurons and structures. The forthcoming secondary injuries outspread to the surroundings, worsening the bedrock of regeneration. Pathological inflammation, ischemia, hemorrhage, edema, and release of reactive oxygen species (ROS) in cells are major causes of further damages[5]. Due to limited recoveries for the axonal regenerative capacity for mitigating the hostile microenvironment in lesion sites, the restoration of neural connectivity across the traumatic area remains difficulties[6]. In addition, the recruited astrocyte-formed hollow cavities impede the restoration and reconnection of the deteriorated nerves. Therefore, the pathological microenvironment is the hindrance of recovery in the central nervous system[7]. Up to now, no effective clinical therapy is listed on guidelines because of the systemic adverse effect in the recovery phase. The blood spinal cord barrier has bordered the therapeutic drug, hampering antibiotic or anti-inflammatory drug accumulation at the target site[8].

It has been reported that natural sources of medications react essentially in pathological microenvironment mitigation[9]. Rutin, a flavonoid phytochemical, can scavenge ROS and reduce the pro-

inflammatory cytokine[10]. Its application in antioxidation, anti-apoptosis, anti-inflammation, and neuroprotection has been confirmed[11–17]. Additionally, a previous study demonstrated that repeated intraperitoneal rutin injections could alleviate spinal cord injury through inhibiting p38 MAPK proteins, and ameliorating oxidative stresses[13]. However, the low solubility, low bioavailability, and the fast clearance limit its application[10].

Exosomes are vesicles (50–150 nm) derived from the luminal membranes of cells and carried with the secreta of original cells, particularly as small molecule drugs, proteins, mRNA, miRNA, etc.[18, 19]. The original role of exosomes is delivering cargos between the membrane-enveloped space for intercellular and intertissue communication[20]. As a delivering vehicle, the exosome essentially uplifts its transportation property for the native biological structure. The conformity between cells and exosomes as bilayer lipid superficial structure and nano-size betters the absorption of medications via membrane fusion and endocytosis. Through undergoing the extraction of *Flos Sophorae Immaturus* leaching solution, the herbal compound as rutin inside mesoderm can be collected in the form of exosomes. Therefore, using exosomes derived from *Flos Sophorae Immaturus* (so-exos) is a solution to the shortcomings of rutin mentioned above.

Furthermore, the pathological microenvironment worsens for weeks, and the fast elimination of nanodrug lowers the therapeutic efficacy[9]. The sustainable release of modulator is demanded in the microenvironment as inflammation and oxidation during rehabilitation. A formerly published article has confirmed the intrinsic therapeutic effect of herbal derived exosomes aiming to regulating gastric bacteria composition and enhancing gut barrier function[20]. However, gastric absorption limits the targeting and accumulation of medications at sites due to the first-pass effect and thus is not suitable for the treatment of SCI. Hydrogels are widely employed in the preclinical treatments of SCI to promote the storage capacity and release profile[21]. Due to the significance and vulnerability of the central nervous system, simulations of the supporting structure and neighboring components of the extracellular matrix can prevent immunologic risks and toxic hazards. Hydrogels' porous and connective traits serve as a platform in the re-distribution and proliferation of local nerve cells. Besides, the bridging effect in the loss area is essential to facilitate the reconnection of spared neurons bilaterally[22]. Hydrogels composed of natural materials have long been used in spinal cord injury treatments. Hyaluronic acid (HA) is broadly adopted due to its biocompatibility, biodegradability, and non-immunogenicity[23].

Herein, a so-exos encapsulated polydopamine (pDA) modified HA hydrogel (pDA-Gel) is implanted in the lesion site to treat acute spinal cord injury. The surrounding hostile ROS environment can be ameliorated through the release of so-exos. Further, so-exos can be uptaken by nerve cells and stimulate its regrowth with a preservative ability. Consequently, the implantation of so-exos encapsulated pDA-Gel in the lesion site enables nerve regeneration and rapid restoration of locomotor function after SCI.

Methods

Reagents and animals

Hyaluronic acids (HA, 1.3 MDa and 2.3 MDa) were purchased from Novozymes (Beijing, China). Dopamine hydrochloride (DA) was acquired from Tansoole Co., Ltd. (Shanghai, China). 2-Amino-2-(hydroxymethyl)-1, 3-propanediol (Tris-HCl, pH 8.5) was purchased from Beyotime (Shanghai, China). Streptomycin, penicillin and 0.25 wt.% trypsin with 0.02 wt.% Ethylene diamine tetraacetic acid (EDTA) were purchased from Gibco BRL (Gaithersburg, MD). High glucose DMEM medium (1×) were purchased from Zhejiang Senrui Co., Ltd. (Huzhou, China).

Female SD rats ranging from 220 g to 250 g used in the SCI model were purchased from SLAC Laboratory Animal Co. Ltd. (Shanghai, China). All animal experiments and procedures were approved and in compliance with the Institutional Animal Care and Use Committee at Zhejiang University.

Fabrication of hydrogel

Basic hydrogel materials were prepared according to previous articles. Briefly, to introduce -CHO at -OH sites of chains, HA (2.3 MDa, 500 mg, 1.25 mmol) was dissolved in ultrapure water (150 mL) and lucifugally oxidized by $NaIO_4$ (10 mg·mL^{-1}) with a mole ratio of 1:0.5 ($NaIO_4$:HA). At the end of 2 continuous days of stirring, the reaction system was stopped by adding ethylene glycol (600 μL) for 1 h. After dialysis, the product was lyophilized and -CHO modified HA (HA-CHO) was obtained. To introduce -NH_2 into HA, adipic dihydrazide (ADH) was utilized as the source. HA (1.3 MDa, 270 mg, 0.675 mmol) and ADH (20.25 mmol, 4.64 g) at a mole ratio of 1:30 (HA:ADH) was dissolved in ultrapure water (150 mL). With an adjusted pH of 6.8, 1-(3-dimethylaminopropyl)-3-ethylcarbodiimide hydrochloride (EDC, 0.96 g, 5 mmol) and 1-hydroxybenzotriazole (HOBt, 0.675 g, 5 mmol) in dimethyl sulfoxide-water (1:1) were added into the reaction system separately. The pH at 6.8 was maintained for the following 4 h and changed to pH 7.0 to end up the reaction. The HA-ADH product was then lyophilized and collected.

Superficial modification of hydrogel

HA-CHO and HA-ADH were dissolved in phosphate buffered saline (PBS) at 20 mg·mL^{-1} and 15 mg·mL^{-1}, respectively. Basic hydrogels were formed with the mixed solution at an equal volume of 30 μL. After placing at 4 ℃ overnight, hydrogel was lyophilized and collected. To further modify the hydrogel, lyophilized hydrogel was swelled in PBS and sterilized under the ultraviolet light overnight. Swelled basic hydrogel were soaked in the polydopamine hydrochloride (pDA) solution at 1 mg·mL^{-1} in Tris buffer (pH 8.5). The superficial modification should take place on an orbital shaker overnight. The pDA-Gel could be obtained through lyophilization.

Characterization of basic hydrogel materials and the modified materials

The lyophilized HA-CHO was stirred with HBr and pulverized into powder for Fourier transform infrared spectroscopy (FTIR) detection to prove the accomplishment of oxidation of carbonyl group at the site of -OH in the product. The HA-ADH modification was confirmed via ^{1}H nuclear magnetic resonance (NMR).

HA-ADH, HA, and ADH were dissolved in deuterium oxide (D_2O). To observe the internal porous structure and superficial modification of the pDA-Gel, scanning electron microscope (SEM) (Nova Nano 450, Thermo FEI, Czech) were used. Both the Gel and the pDA-Gel were sliced and covered with gold in vacuum for examination.

Isolation of Sophora exosomes (so-exo)

All *Flos Sophora Immaturus* were bought from markets. Most of so-exos were naturally stored in the mesoderm of *Flos Sophora Immaturus*. To prepare so-exos, appropriate sinking buffer was required to penetrate the outer face and permeate the whole mesoderm of plant so as to swell the plant cell. 4-Morpholine ethanesulfonic acid (MES) buffer was known as preservation of antioxidant factors in plants. After sinking the sophora in MES buffer (pH 6.0) for 24 h, the extracted juice was collected from swelled sophora via centrifugation at 2000 g for 20 min. The rough purification of soak extraction was employed through centrifugation at 3000 g and 10000 g for 30 min each to remove cells and debris. The fine purification of supernatant was employed through centrifugation at 100000 g for 70 min twice and an extra PBS resuspension centrifugation. Pelleted so-exos were resuspended in 300 μL PBS. All purification was under the condition of 4 ℃.

Characterization of so-exos

Structural morphology and size confirmation were affirmed via transmission electron microscopy (TEM). 5 μL of so-exo solution was added on formvar/carbon-coated 200-mesh copper electron microscopy grids. After incubation at room temperature for 3 min, standard uranyl acetate staining was performed to fix the whole structure. Before the TEM observation, grids were semi-dried at room temperature.

Quantification and labeling of so-exos

Rutin components inside so-exos were detected by high performance liquid chromatography (HPLC, Agilent Technologies 1200 series). Rutin was detected by photo-diode array detector at 257 nm. The chromatographic column was C_{18} column (5 μm, 150 mm×4.6 mm) (Diamonsil, Dikma, China). The mobile phase was methanol: 1% glacial acetic acid solution, 40:60; Flow rate should be 1 $mL \cdot min^{-1}$; Temperature was 25 ℃. Micro BCA protein assay kit (Thermo Fisher Scientific, USA) was used to detect exosome concentration. The ratio between rutin dosage, particle number and protein content were calculated through conversion.

Adhesive ability of so-exos

Both Gel and pDA-Gel were fully swelled in PBS and sterilized under ultraviolet overnight. Gels were washed with 75% ethyl alcohol and PBS for further sterilization. So-exos were resuspended in PBS to a concentration of 5 $mg \cdot mL^{-1}$. Each gel was injected with 20 μL of so-exo suspension. Incubation of the so-exos encapsulated gel was conducted at 37 ℃ for 1 h and at 4 ℃ overnight to strengthen the adhesiveness of exosomes as far as possible. Thus, so-exos encapsulated hydrogels were fully prepared for adhesive ability analysis and *in vivo* implantation. As for adhesive ability analysis, former prepared gels were carefully sunk in PBS for 5 min and rinsed with PBS twice the next day. Afterwards, gels were

diluted to 250 μL and vibrated in ultrasound. Once more, vibration was employed to ensure the full extraction of encapsulated exosome. Protein amounts were detected via micro BCA. Blank gel group injected with PBS should be set up to eliminate the material disturbance. As for *in vivo* implantation, gels were prepared 1 day before the SCI model establishment.

Evaluation of cellular viability, intercellular ROS level and adenosine triphosphate (ATP) activity

SH-SY5Y cells were cultured in high glucose DMEM medium containing 10% FBS, 1% penicillin and streptomycin (100×) with 5% CO_2 at 37 ℃. To evaluate cellular viability after diverse treatments, cells were seeded in 96-well plates (5000 cells per well). After the attachment of cells on the plate bottom, medium was replaced with fresh FBS-free medium containing so-exos, rutin with a gradient rutin concentration (0.5, 0.25, 0.125 mg·mL^{-1}). After 24 h incubation under hypoxia condition (1% O_2, 5% CO_2, 37 ℃), the plate was rinsed with FBS-free medium. The cell counting kit-8 (cck8) was used to evaluate the cell viability and the detection was manipulated at 450 nm.

The intercellular ROS level was tested using 2,7-dichlorodi-hydrofluorescein diacetate (DCFH-DA) as the ROS detector. After incubation and rinse, cells were incubated with 1:1000 DCFH-DA in FBS-free medium at 37 ℃ for 20 min. The detection was manipulated on SpectraMax M5 (Molecular Devices, USA) after rinsing. The excitation and emission wavelengthes were 488 and 525 nm respectively. The ATP activity evaluation was tested via ATPase test kit. After the removal of medium, each well was added 200 μL of cell lysis buffer. After disassociation by repeatedly pipetting, cells were centrifugated at 12000 g for 5 min. The supernatant was preserved for further detection. Supernatant were tested with working fluid according to the kit procedure. Thus, luminance can be detected by fluorescence spectrophotometer (E6080, Promega Company). All ATP detection procedures were done at the temperature of 4 ℃.

Surgical procedure for spinal cord transection model and so-exo + pDA-Gel implantation

Rat SCI model was prepared through transection over spinal cord with a lesion about 4.0 ± 0.5 mm as previously mentioned[24]. Under deep anesthesia, hair on the back of the rats near their T10 spinous processes was shaved. With the separation of muscle, laminectomy was performed to expose spinal T9-T11 segments. A complete transection between the T9-T10 segment made a lesion gap of 4.0 ± 0.5 mm. So-exos + pDA-Gel was implanted between the gap of lesion site after hemostasis. SCI, pDA-Gel and rutin + pDA-Gel group were administrated in the same way to serve as groups for comparison. Animals receiving the same surgical procedure without spinal cord transections were set as sham group. Preparation of so-exo encapsulated gel is manipulated as previous experiment. In brief, so-exos were pipette into gels and incubated overnight. After the implantation, muscle and skin were separately sutured. Penicillin was intermuscular injected within 7 days after the surgical procedure. For better prognosis and restoration of urinary function, manual bladder massage was conducted twice daily until the micturition reflex recovery.

Locomotor function investigation

The postsurgical analysis of locomotor behavior was valuated weekly. Unrestrainedly, animals were moving in an open field, and were graded according to the 21-point Basso, Beattie, Bresnahan (BBB) locomotion rating scale by observers blinded to treatment group for each animal. Since all graded videos of rats were recorded, observers can repeatedly review the moving condition of each rat.

Sacrification for tissue, Hematoxylin and eosin (HE) and immunohistochemistry staining

Rats were sacrificed at the end of treatment experiment (Day 28) under deep anesthesia. Whole body were firstly perfused by isotonic physiological saline and then by 4% paraformaldehyde in PBS. Spinal cords surrounding the lesion site as well as major organs (hearts, livers, spleens, kidneys and bladders) were collected. The harvested tissues from each group were dehydrated in processing cassettes through a series of alcohol gradient overnight. After embedding, the section slices were stained according to HE staining kit. For immunofluorescence staining of the spinal cords, tissues were embedded and cryosectioned into 20 μm slices. After permeabilizing with Triton X100, sliced tissues were incubated with antibodies as neurofilament (NF) (Cell Signaling Technology, USA), glial fibrillary acidic protein (GFAP) (Boster, China), 4-hydroxynonenal (4-HNE) (Omnimabs, USA), 8-hydroxy-2’-deoxyguanosine (8-OHdG) (Omnimabs, USA) and choline acetyl transferase (ChAT) (Omnimabs, USA) overnight at 4 ℃. After rinsing with primary antibodies, the sections were incubated with Alexa Fluor 488- and 594-conjugated secondary antibodies (Jackson ImmunoResearch, USA) at 37 ℃ for 30 min. Nuclei were labeled via DAPI staining (Invitrogen, USA). The sections were observed using Olympus SLIDEVIEW VS200 (VS200, Olympus, USA).

Statistical Analysis

The quantitative results were shown as mean ± standard deviation values. Statistical analysis was calculated through GraphPad prism 8.4. Two-tailed unpaired t-test and one-way ANOVA were used under normal distribution and variance homogeneity. Significance can be proven by a P-value lower than 0.05.

Results

Characterization of so-exos and capacity optimization of hydrogel

So-exos were collected through formerly mentioned protocols (Fig. 1A). With the help of soak and repeated centrifugation, purification was done in the meanwhile. The sediment should be resuspended and collected in PBS and can be recognized as purified so-exos. Purified so-exos were sterilized through percolating via a 0.22 μm microfiltration membrane for further cellular manipulation. TEM and nanoparticle tracking analysis (NTA) confirmed the so-exos morphology and the size distribution. Results from TEM and NTA demonstrated that so-exos had a cup shape (Fig. 2B) with a diameter of 151 nm

(Fig. 1C). Thus, the size qualifies the classic exosome standard ranging from 50–200 nm. Rutin was defined as the critical therapeutic and referring component in the following experiment. Interior components of so-exos such as rutin need to be identified and quantified through HPLC. It has been recognized as rutin since the retention time of the reference standard and that in so-exos matched each other (Fig. 1D). The quantification of rutin was determined by a standard linear curve. To clarify the modification results as HA was modified with aldehyde and adipic dihydrazide, ^{1}H NMR and FTIR analysis were utilized (Fig. 1E & 1F). Click chemical reaction between aldehyde and amino group formed the Gel. For continued stimulation, sustainable release of lipid-structure exosome required an adherent feature. With the demand for higher adhesiveness of Gel, pDA covered the former fabricated Gel and optimized it as pDA-Gel (Fig. 1G).

After the fabrication of Gel and pDA-Gel, physical characteristics were analyzed through SEM. SEM illustrated the appearance of Gel and pDA-Gel (Fig. 1H). Superficially, pDA-Gel offered a smoother surface and enhanced the adhesiveness. After incubating so-exos in hydrogels, so-exos can be trapped in its porous structure. SEM demonstrated that pDA-Gel could easily load so-exos compared with basic Gel. Large amounts of exosomes in pDA-Gel were restrained and adhered to the surface, while those in basic Gel can hardly reside after repeated rinsing. The adhesive capability of hydrogel improved the carrying ability of so-exos compared to the original Gel.

In vitro protective capability of so-exo under hypoxia condition

After SCI, numerous ROS and inflammatory factors were released in the lesions locally. Under long-term hypoxic conditions, insufficient oxygen content in cells would transform and deform the cell mitochondria. Mitochondria would spontaneously release ROS molecules afterward, further weakened cell proliferation and increased apoptosis. Therefore, it is of great importance to maintain cell viability in a rigorous environment. As shown in Fig. 2A and Fig. 2B, there was no difference in the effect of so-exos and rutin on cell proliferation under normal oxygen conditions (Fig. 2A), while so-exos could ameliorate cell damage in hypoxia (Fig. 2B). Exosomes have better preservation capability in cellular viability than rutin at the same concentration. At the same time, the live/dead staining results were consistent with the results of cell viability evaluated by cck8 test (Fig. 2E). The preservative ability of so-exos is evidant when facing the ROS environment. However, neither forms exhibited the concentration dependence. Subsequently, according to the results of the antioxidant evaluation, so-exos could effectively decrease the level of intracellular ROS compared with rutin of the same concentration (Fig. 2C). Further evaluation showed that under hypoxia, so-exos could prevent the decrease of cell ATPase activity (Fig. 2D). Therefore, these results indicate that the increase of cell activity in hypoxic conditions might be related to the antioxidant function of so-exos, which is beneficial for ameliorating damages caused by the intercellular ROS microenvironment on ATPase in mitochondria.

In this study, there is no concentration-dependent effect in cell viability and ROS level because of the balance between toxicity and therapeutic effect. Pharmaceutical concentration at 0.25 $\mu g \cdot mL^{-1}$ is the

best fit for the number of cells and ROS level. Also, the ROS levels in the higher concentration rutin group is elevated.

In vivo protective capability of so-exos via ROS cleavage after SCI

In order to evaluate outcomes on regulating the microenvironment, rats are divided into four groups. SCI model group, pDA-Gel group, and rutin + pDA-Gel group were set up as control groups. Rats in SCI model group were only given PBS. Rats in rutin + pDA-Gel group were given pDA-Gel injected with the same amounts of rutin and solution compared to so-exos solution. So-exo + pDA-Gel group was set up as a test group, while rats in that group were given pDA-Gel injected with so-exos. On Day 28 post-surgery, all animals were sacrificed and their spinal cords in 4 groups were collected. First, neurofilaments and astrocytes were stained so as to evaluate the nerve regeneration and astrocyte recruitment.

Generally, the innertissue hollow cavity could be seen in SCI model group. The nerve regrowth starts at the edge of hydrogels in the implanted group. Bridging effect and tissue continuity can be identified within the local area. The distribution of neurofilaments (NFs) and glial fibrillary acidic protein-positive ($GFAP^+$) astrocyte, a glial scars marker, is related to the extent of regeneration. The participation of $GFAP^+$ astrocytes inhibit neurofilament proliferation. The combinational therapy prevents astrocytes aggregation to promote nerve proliferation. More amounts of astrocytes can be seen in SCI model compared to the combinational treatment group (Fig. 3A). The fewer $GFAP^+$ astrocytes locate, the more proliferation triggers in the local area. The evaluation of the choline acetyltransferase (ChAT), a neurotransmitter enzyme mainly found in cholinergic neurons, demonstrated the unanimous result as neurofilament. General restoration of ChAT was found in the so-exo + pDA-Gel group indicating the connectivity of neurons in the lesion site (Fig. 3B). Though peroxides could still be detected in so-exo + pDA-Gel group slices, it was lower than other groups. The sustainable releasing ability can ameliorate the surrounding ROS, which is potential for further structural recovery (Fig. 3C). In conclusion, the combinational therapy as so-exo + pDA-Gel demonstrates its anti-ROS, nervous restoration ability and bridging effects *in vivo*.

Functional and histological restoration of locomotive and urinary system via so-exos

Rats were randomly categorized into five groups as Sham, SCI, pDA-Gel, rutin + pDA-Gel, and so-exo + pDA-Gel. The comparison among pDA-Gel, rutin + pDA-Gel, and so-exo + pDA-Gel was conducted to assess the efficacy of the encapsulated so-exos, while rutin can serve as a comparative positive reference under equal dosage. Animals that underwent deep anesthesia, haircut, and laminectomy without any transactions served as Sham group. Moreover, animals experiencing all surgical procedures and receiving only PBS rinsing in lesion sites served as the SCI group. The Investigation of Sham and SCI groups were mainly for pathological overview and functional assessment. Spinal cord injury models were established using the formerly mentioned method. We massaged post-operative rat bladders for four weeks and injected penicillin intramuscularly for a week. Videotaping ought to be taken every week to observe the

recovery of the motor system (Fig. 4A). Since SCI was established, severe motor system dysfunction and paralysis were shown among the nontreated rats during the past 28 days.

In contrast, the therapeutic groups revitalized the motor function, especially the combinational group (so-exo + pDA-Gel). The motor system evaluation is mainly based on the BBB scores analysis. Double-blinded evaluations were used in order to avert subjective opinions. Animals in the combinational therapeutic group demonstrated a significant improvement in the motor system and had a BBB score of 6.00 ± 0.70 after a 28-day recovery, which is superior to that of the SCI group (2.00 ± 0.00) (Fig. 4B). The conclusion of BBB scores shows significant behavioral changes in the so-exo + pDA-Gel group compared with all other groups since week 1. However, no evident improvements were found in other therapeutic groups. The behavioral improvement could be solid evidence of nerve conduction recovery. Further, the bettering was elevated every week and intended to be stable between week 3 and 4. Video observation demonstrated that hindlimbs had an extensive movement of two joints and slight movement of the third, while sometimes had an extensive movement of all three joints. There was a significance shown between the combinational therapeutic group and the SCI model group. As for rutin group, no obvious improvement can be observed. An additional movie file shows this in more detail [see Additional file 1]. The direct delivery of rutin without sustainability cannot significantly uplift autonomic and motor functions. Compared to the combinational therapeutic group, the hindlimbs in SCI group could merely sweep the floor and symptom of paraplegia. However, since no weight-supported hindlimb movement was shown in floor walking, no significance can be seen in the horizontal ladder rung walking test. As a result, the group of animals implanted with so-exo + pDA-Gel demonstrated its effective restoration of the motor system. The combinational therapeutic group has illustrated its potential in nerve regeneration and functional recovery.

Furthermore, there was an obvious complication after the SCI model establishment as urinary retention. Continuous urinary retention would lead to general pathological hyperplasia as well as a secondary infection. The bladder is the primary organ that faces urinary dysfunction. Thus, both histological and functional changes could be observed in the bladder of the rats in the SCI group. The recovery and restoration of bladders can be side proofs of therapeutic effect. HE staining of the bladder presented hyperplasia both in the muscular layer and epithelium layer, which were thicker compared to those in the Sham group. More pus cells could be seen in the epithelium layer of the SCI model group, demonstrating the secondary infection was much more severe in the SCI group (Fig. 4D). In contrast, pathological accommodation would disappear faster with the recovery of the locomotor system and nerve conduction. The transitional epithelium of bladders in the therapeutic group stayed intact and multi-layer structure while that in the SCI group was deformed into the single-layer structure. Since the dynamic urinary tract obstruction and establishment of lower-level nerve circuit in spinal neurons, bladders' contraction function should be strengthened to pump out the excess urine. Masson staining shows bladders in the SCI model group have hyperplasia in both muscle bundle and collagens. The thickness differences were evident among groups. The urine retention phenomenon in the combinational therapy group, the so-exo + pDA-Gel group, was not as severe as the SCI model group. Thus, it is another evidence of nerve restoration and conduction recovery in related organs. HE staining of main organs such as kidney, heart,

liver, and spleen were further studied for evaluating pharmaceutical safety. Results illustrated that no significant change was observed in the kidneys except for slight edema in the nephron. Other than the urinary system, cardiovascular, hepatic systems and spleens were not significantly changed (Fig. 4E). Muscular cells, hepatic lobules, white pulps and red pulps have shown no differences in histology and morphology. No apparent dysfunction and notable pathological alteration were seen among all groups. This result offers a safety profile of components of therapies.

Discussion

Traumatic injuries in the central nervous system are always deteriorated by secondary damage. Microglia-derived extracellular ROS act as stimuli for further damages in neurodegenerative and neurotoxic diseases[25]. The secondary period damages detriments the surrounding nerve tissues by expressing inflammatory factors, elevating the ROS, and forming glial scar barriers. The oxidative stress in the lesion sites is the major hazardous factor in secondary injury. The amounts of ROS are correlated to the treatment outcome. Effective strategies that inhibit further oxidative injury have shown a significant treating result for SCI[24]. Furthermore, the regeneration of the central nervous system is not only based on the hazardous factor cleavage but also proliferative bedrock. Implantation as hydrogels plays a depot-like and scaffold-like role that offers sustainability and bridging ability. Numerous researchers in the past few years developed biomaterials scaffolds engaging in biophysical therapy[26–28]. However, simple scaffolds cannot satisfy the requirement in both nutritional and regenerative effects. Here a novel combinational therapy was designed towards spinal cord injury, aiming to reconstruct the nerve connectivity, nourish starved tissue, and elevate regeneration outcomes.

Rutin, as natural medicine, is proved to ameliorate ROS levels by inhibiting the p38 MAPK pathway. The p38 MAPK pathway is recognized as a pro-inflammatory and pro-oxidant signal in the nervous system[13]. Oxidative stress is related to the activation of mitochondria in microglia in the CNS. It has also been proved that p38 MAPK signal inhibition can promote the autophagy of microglia and silence the activated microglia[29]. Though rutin can promote nerve regeneration and ROS cleavage by inhibiting p38 MAPK pathway, the blood-brain barrier constrained therapeutics accumulation *in situ* and concentration maintenance during recovery[30, 31]. Plant exosome discharging from *Flos Sophora Immaturus* encapsulated in hydrogel provides an innovative means to figure out the drawbacks mentioned above. Moreover, exosome is recognized as a vital drug and genetic transportation for intercellular communication[32]. Due to the similarities of the lipid bilayer, endocytosis promotes so-exos cellular uptake[33]. Well accumulation and effective uptake synergistically uplift the cleavage of the ROS microenvironment and restoration of locomotive and nervous system. Furthermore, compared to mammalian exosomes, plant exosomes have gigantic quantity in treatment and potential in research field. With the further study of their intrinsic mechanism, plant exosome provides a promising alternative in future treatment.

This study presents a novel combinational therapy for spinal cord injury, based on *Flos Sophora Immaturus* derivatives as so-exos accompanied with high-adhesive pDA-covered hydrogels. The combinational implantation, also known as so-exo + pDA-Gel, can sustainably release exosomes into the surrounding lesion area. Proliferation and restoration of spinal nerves were shown during 28 days implantation placing treatment. Functional and histological recoveries were demonstrated between SCI group and the so-exo + pDA-Gel group. Through microenvironment regulation, dysfunctional locomotor system and damaged nerve tissues were tremendously recuperated, exhibiting the remarkable potential of sustainable plant exosome release in tissue repair. Consequential urinary system damages to bladders and kidneys were mitigated through expeditious neuronal rejuvenation. Accordingly, we here to display an innovative combinational treatment based on plant derivatized exosomes adhering to pDA-decorated hydrogels implantation for the potent and proliferative treatment in CNS diseases and limited tissue regeneration.

Conclusion

We used so-exo + pDA-Gel as a combinational therapy to deliver plant exosome derived from *Flos Sophora Immaturus* to improve SCI prognoses. Our findings demonstrate that rutin carried exosomes encapsulated in hydrogels can lower ROS levels *in situ* and preserve mitochondria from ROS accumulations. Consequently, this approach could successfully improve the post-SCI condition and facilitate nervous connectivities.

List Of Abbreviations

SCI Spinal cord injury

pDA Polydopamine

pDA-Gel Polydopamine modified hydrogel

ROS reactive oxygen species

So-exos Exosomes derived from *Flos Sophorae Immaturus*

HA Hyaluronic acid

TEM Transmission electron microscopy

NTA Nanoparticle tracking analysis

NFs Neurofilaments

GFAP+ Glial fibrillary acidic protein-positive

ChAT Choline acetyltransferase

HE Hematoxylin and eosin

Declarations

Ethics approval and consent to participate

All animal experiments and procedures were approved and in compliance with the Institutional Animal Care and Use Committee at Zhejiang University.

Consent for publication

Not applicable

Availability of data and materials

Data sharing is not applicable to this article as no datasets were generated or analysed during the current study.

Competing interests

The authors declare that they have no competing interests.

Funding

This work has been financially supported by the National Key Research and Development Project of Stem Cell and Transformation Research (2019YFA0112100), National Natural Science Foundation of China (81973252).

Authors' contributions

Liming Li and Jianqing Gao initiated the idea, designed the experiments, supervised the research. Jiachen Chen, Jiahe Wu wrote the manuscript. Jiachen Chen and Jiafu Mu performed most of the experiments. Jingyi Hu, Hangjuan Lin, and Jian Cao discussed the results and provided critical reagents. All authors read and approved the final manuscript.

Acknowledgements

We thank the Center of Cryo-Electron Microscopy (CCEM), Zhejiang University, for the technical assistance on Confocal Laser Scanning Microscopy and Scanning Electron Microscopy. We thank the Center of Protein, Zhejiang University, for the technical assistance on Ultracentrifuge. We thank Jianyang Pan (Research and Service Center,College of Pharmaceutical Sciences, Zhejiang University) for performing NMR spectrometry for structure elucidation.

References

1. Holmes D. Spinal-cord injury: spurring regrowth. *Nature*. 2017;552(7684):S49.
2. Collaborators GN. Global, regional, and national burden of neurological disorders, 1990-2016: a systematic analysis for the Global Burden of Disease Study 2016. *The Lancet. Neurology.* 2019;18(5):459-480.
3. Wyndaele M, Wyndaele J. Incidence, prevalence and epidemiology of spinal cord injury: what learns a worldwide literature survey? *Spinal Cord.* 2006;44(9):523-529.
4. Koffler J, Zhu W, Qu X, et al. Biomimetic 3D-printed scaffolds for spinal cord injury repair. *Nat Med.* 2019;25(2):263-269.
5. Hutson TH, Di Giovanni S. The translational landscape in spinal cord injury: focus on neuroplasticity and regeneration. *Nature reviews. Neurology.* 2019;15(12):732-745.
6. Cowan H, Lakra C, Desai M. Autonomic dysreflexia in spinal cord injury. *BMJ (Clinical research ed.).* 2020;371:m3596.
7. Vismara I, Papa S, Rossi F, Forloni G, Veglianese P. Current Options for Cell Therapy in Spinal Cord Injury. *Trends Mol Med.* 2017;23(9):831-849.
8. Gabathuler R. Approaches to transport therapeutic drugs across the blood–brain barrier to treat brain diseases. *Neurobiol Dis.* 2010;37(1):48-57.
9. Dad HA, Gu T, Zhu A, Huang L, Peng L. Plant Exosome-like Nanovesicles: Emerging Therapeutics and Drug Delivery Nanoplatforms. *Molecular therapy : the journal of the American Society of Gene Therapy.* 2021;29(1):13-31.
10. Cosco D, Failla P, Costa N, et al. Rutin-loaded chitosan microspheres: Characterization and evaluation of the anti-inflammatory activity. *Carbohyd Polym.* 2016;152:583-591.
11. Pan RY, Ma J, Kong XX, et al. Sodium rutin ameliorates Alzheimer's disease-like pathology by enhancing microglial amyloid-beta clearance. *Sci Adv.* 2019;5(2):eaau6328
12. Tasli NG, Ucak T, Karakurt Y, et al. The effects of rutin on cisplatin induced oxidative retinal and optic nerve injury: an experimental study. *Cutan Ocul Toxicol.* 2018;37(3):252-257.
13. Song H, Zhang X, Wang W, et al. Neuroprotective mechanisms of rutin for spinal cord injury through anti-oxidation and anti-inflammation and inhibition of p38 mitogen activated protein kinase pathway. *Neural Regen Res.* 2018;13(1):128-134.
14. Nkpaa KW, Onyeso GI, Kponee KZ. Rutin abrogates manganese-Induced striatal and hippocampal toxicity via inhibition of iron depletion, oxidative stress, inflammation and suppressing the NF-kappaB signaling pathway. *J Trace Elem Med Biol.* 2019;53:8-15.
15. Guimaraes JF, Muzio BP, Rosa CM, et al. Rutin administration attenuates myocardial dysfunction in diabetic rats. *Cardiovasc Diabetol.* 2015;14:90.
16. Alonso C, Rubio L, Tourino S, et al. Antioxidative effects and percutaneous absorption of five polyphenols. *Free Radic Biol Med.* 2014;75:149-155.
17. Habtemariam S. Antioxidant and Rutin Content Analysis of Leaves of the Common Buckwheat (Fagopyrum esculentum Moench) Grown in the United Kingdom: A Case Study.

Antioxidants. 2019;8(6):160.

18. Tran PHL, Xiang D, Tran TTD, et al. Exosomes and Nanoengineering: A Match Made for Precision Therapeutics. *Adv Mater.* 2019:1904040.
19. Vader P, Mol EA, Pasterkamp G, Schiffelers RM. Extracellular vesicles for drug delivery. *Adv Drug Deliver Rev.* 2016;106(Pt A):148-156.
20. Teng Y, Ren Y, Sayed M, et al. Plant-Derived Exosomal MicroRNAs Shape the Gut Microbiota. *Cell Host Microbe.* 2018.
21. Wang W, Lu K, Yu C, Huang Q, Du Y. Nano-drug delivery systems in wound treatment and skin regeneration. *J Nanobiotechnol.* 2019;17(1):82.
22. Chen J, Li L, Gao J. Biomaterials for local drug delivery in central nervous system. *Int J Pharmaceut.* 2019;560:92-100.
23. Li L, Zhang Y, Mu J, et al. Transplantation of Human Mesenchymal Stem-Cell-Derived Exosomes Immobilized in an Adhesive Hydrogel for Effective Treatment of Spinal Cord Injury. *Nano Lett.* 2020;20(6):4298-4305.
24. Li L, Zhang Y, Mu J, et al. Transplantation of Human Mesenchymal Stem-Cell-Derived Exosomes Immobilized in an Adhesive Hydrogel for Effective Treatment of Spinal Cord Injury. *Nano Lett.* 2020.
25. Simpson DSA, Oliver PL. ROS Generation in Microglia: Understanding Oxidative Stress and Inflammation in Neurodegenerative Disease. *Antioxidants (Basel, Switzerland).* 2020;9(8).
26. Zhou L, Fan L, Yi X, et al. Soft Conducting Polymer Hydrogels Cross-Linked and Doped by Tannic Acid for Spinal Cord Injury Repair. *Acs Nano.* 2018.
27. Li L, Huang L, Jiang X, Chen J, OuYang H, Gao J. Transplantation of BDNF Gene Recombinant Mesenchymal Stem Cells and Adhesive Peptide-modified Hydrogel Scaffold for Spinal Cord Repair. *Curr Gene Ther.* 2018;18(1):29-39.
28. Zhang Y, Li L, Mu J, Chen J, Feng S, Gao J. Implantation of a functional TEMPO-hydrogel induces recovery from rat spinal cord transection through promoting nerve regeneration and protecting bladder tissue. *Biomater Sci.* 2020;8(6):1695-1701.
29. Block ML, Zecca L, Hong J. Microglia-mediated neurotoxicity: uncovering the molecular mechanisms. *Nature reviews. Neuroscience.* 2007;8(1):57-69.
30. Abbott NJ, Rönnbäck L, Hansson E. Astrocyte–endothelial interactions at the blood–brain barrier. *Nat Rev Neurosci.* 2006;7(1):41-53.
31. Huang L, Hu J, Huang S, et al. Nanomaterial applications for neurological diseases and central nervous system injury. *Prog Neurobiol.* 2017;157:29-48.
32. El-Andaloussi S, Lee Y, Lakhal-Littleton S, et al. Exosome-mediated delivery of siRNA *in vitro* and *in vivo*. *Nat Protoc.* 2012;7(12):2112-2126.
33. Barile L, Vassalli G. Exosomes: Therapy delivery tools and biomarkers of diseases. *Pharmacol Therapeut.* 2017;174:63-78.

Scheme

Scheme 1 is available in the Supplemental Files section.

Figures

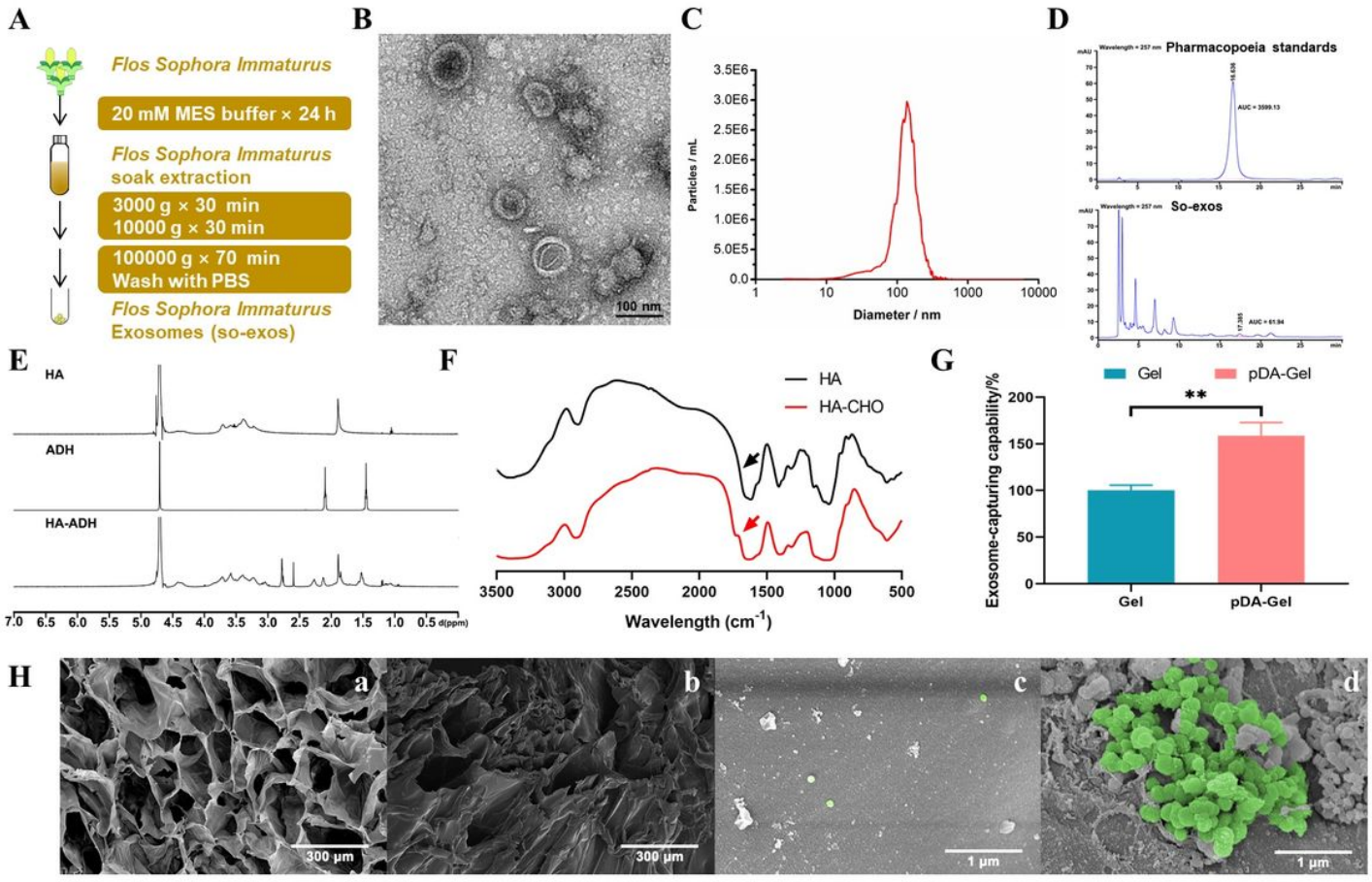

Figure 1

Preparation and characterization of so-exo and pDA-Gel. (A) Schematic illustration of so-exos reparation protocol. (B) TEM micrograph of purified so-exos. (C) NTA counts for the particle size distribution of so-exos. (D) Identification and quantification of rutin in the purified so-exos. (E) ^{1}H NMR spectra of HA-ADH, ADH and HA, respectively. (F) FTIR spectra of HA-CHO and HA, respectively. Arrows point out the absorption peak differences of the carbonyl group. (G) The adhesiveness of so-exos in Gel or pDA-Gel after incubation for 24 h. (H) SEM micrographs of the highly porous inner structure and superficial smooth coverage of Gel (a) and pDA-Gel (b). SEM micrographs of the superficial structure of Gel (c) and pDA-Gel (d) after incubation with so-exos.

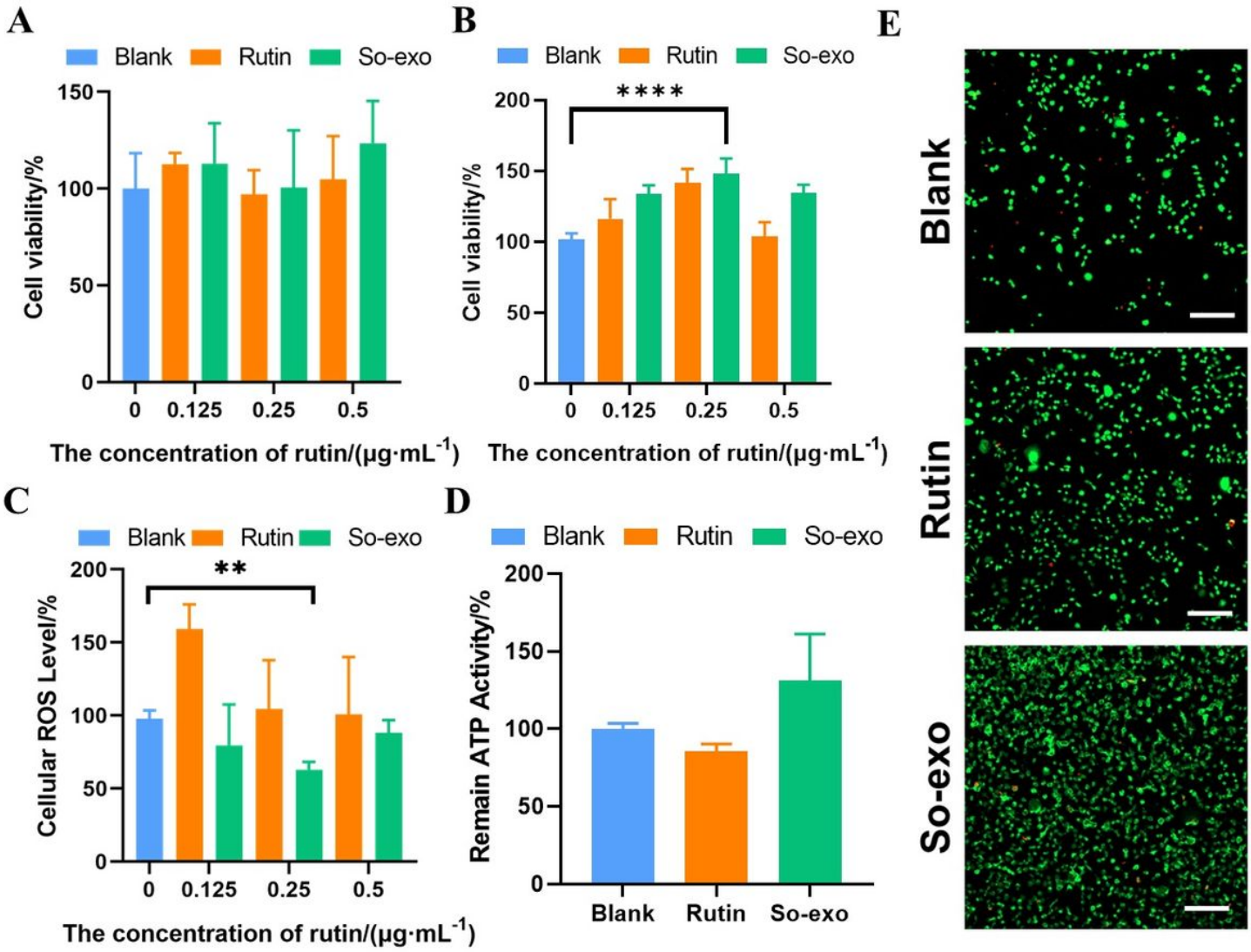

Figure 2

Evaluation of ROS scavenging and cellular protection effect of so-exos under hypoxia condition. (A) Cell viability of SH-SY5Y under normal oxygen condition incubated with rutin and so-exos. (B) Cell viability of SH-SY5Y under hypoxia condition incubated with rutin and so-exos. (C) Comparison of ROS scavenging ability between rutin and so-exo combating 100 μM H_2O_2 solution through DCFH-DA test kit. (D) Cellular ATP activity stimulated by rutin or so-exos were detected through ATP assay kits. (E) Live/Dead staining of the cells after incubation with rutin or so-exos under hypoxia, visualized by the confocal laser scanning microscope. Scale bar, 200 μm. Significance was marked as ** for $P < 0.01$, **** for $P < 0.0001$.

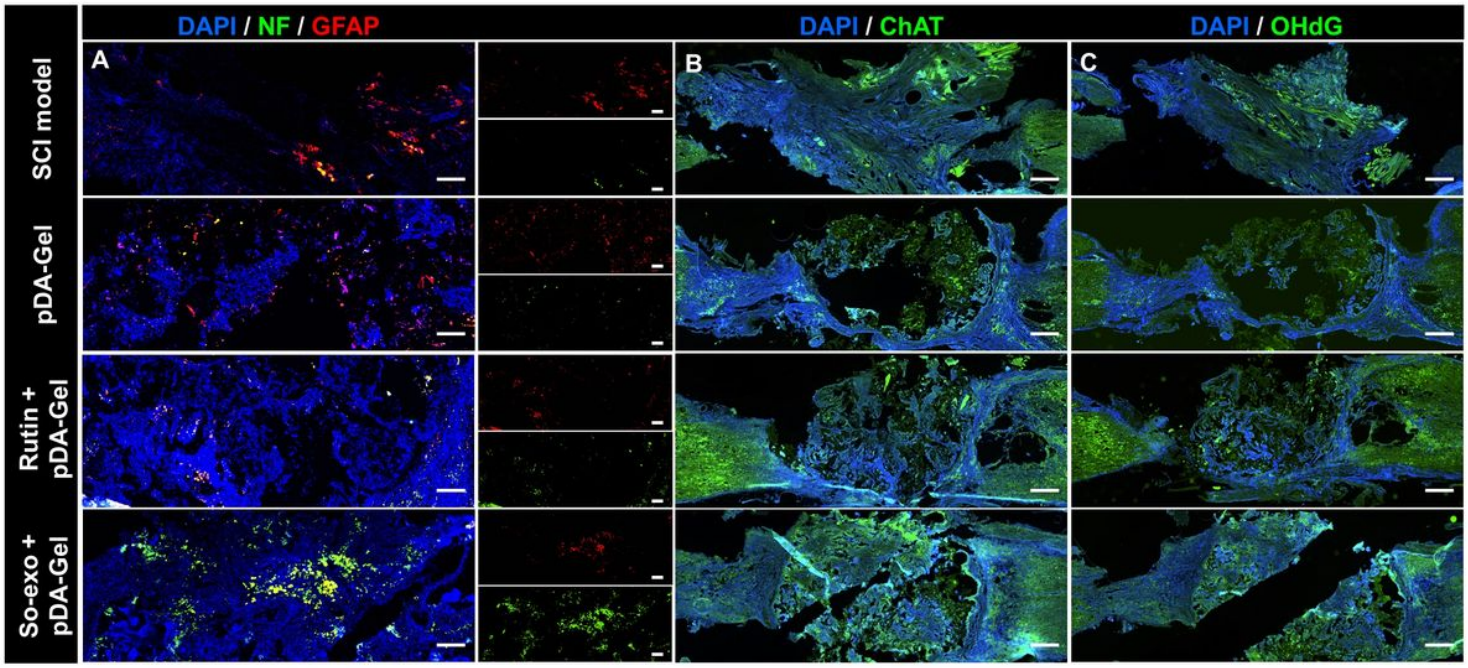

Figure 3

Regeneration of nerve cells and cleavage of ROS by combinational therapy *in vivo*. On Day 28 post surgery, all sections were spinal cords harvested from SCI model group, pDA-Gel group, rutin+pDA-Gel group, and so-exo+pDA-Gel group. (A) Representative images illustrate neurofilaments (NF, green) and glial fibrillary acidic protein (GFAP, red) and nuclei (blue). (B) Regeneration of nerve cells were marked with choline acetyltransferase (ChAT, green) so as to demonstrate cholinergic neurons. (C) The cleavage of ROS factor was confirmed by staining with 8-hydroxy-2-deoxyguanosine (8-OHdG, green). Scale bars in figure 3A is 200 μm, and those in figure 3B & 3C are 500 μm.

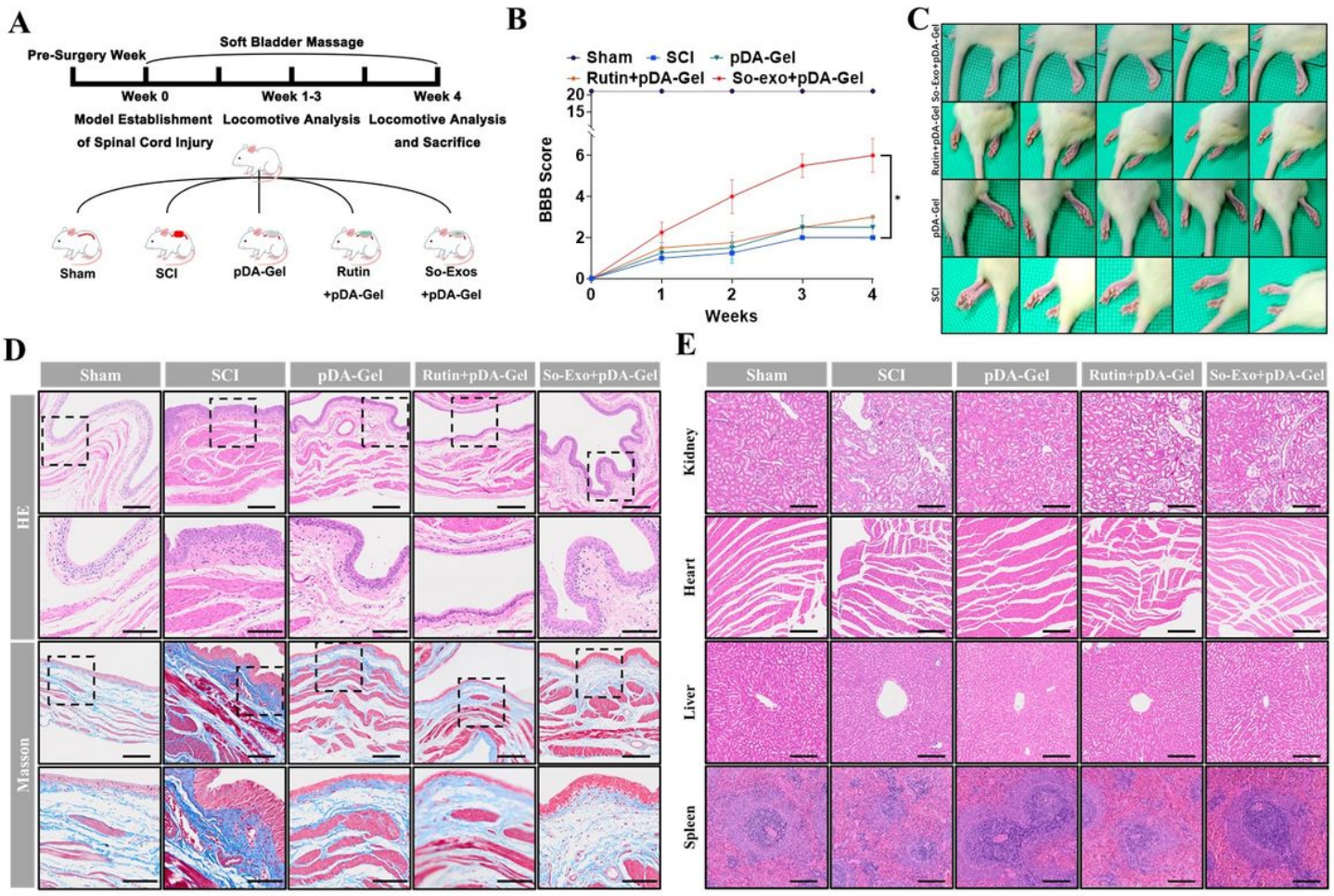

Figure 4

Functional restoration analysis. According to the experiment design and classification (A), rats were randomly distributed into categories and conformed to procedures. Each rat would be videotaped and analyzed every week. The locomotive system recovery result can be concluded into BBB scores (B) by their performance. Videotapes were interpreted into BBB scores and captured into frames to demonstrate their movement on day 28 (C). (D) were hematoxylin and eosin (HE) and Masson staining of bladders on Day 28 post-surgery. The boxed images were further demonstrated as the magnified view of fields under the regular frame. (E) Biosafety evaluation of main organs as hearts, livers, spleens and kidneys from different groups was analyzed via HE staining. Except for scale bars in the second and fourth row in (D) were 100 μm, all other scale bars were 200 μm. Significance was marked as * for $P < 0.05$.

Supplementary Files

This is a list of supplementary files associated with this preprint. Click to download.

- Additionalfile1.mp4
- Scheme1.jpg